

Comparative Study of the Condition for Non-Oscillatory Solution of a Singularly Perturbed Problem on Uniform and Piecewise-Uniform Meshes


Aslam Abdullah^{1,*}

¹ Department of Aeronautical Engineering, Faculty of Mechanical and Manufacturing Engineering, Universiti Tun Hussein Onn Malaysia, 86400 Parit Raja, Johor, Malaysia

ARTICLE INFO

Article history:

Received 21 June 2020

Received in revised form 20 August 2020

Accepted 25 August 2020

Available online 31 August 2020

Keywords:

Uniform mesh; piecewise-uniform mesh;
 Shishkin mesh; singularly perturbed
 problem; finite difference method

ABSTRACT

Wide range of mesh types are proposed in computational fluid dynamics which in turn initiate further discussions over problems of their structure in the numerical computation of fluid flows. Nevertheless, such discussions might sometimes lead to ill-fitted choices of mesh for specific problem. Some types, if improperly used, can cause spurious oscillation in the solutions of governing equations. Furthermore, the contribution of mesh and flow parameters in predicting spurious oscillation free solutions has been much-debated topic over the last decades. Comparison was made in this research between uniform and piecewise-uniform meshes in accentuating the significance of the mesh structure and singular perturbation parameter connection in numerical solution of a singularly perturbed problem. A systematic technique was particularly applied in setting both the singular perturbation parameter and mesh number. Based on the a priori formulation, the condition to avoid spurious oscillatory solutions on the two types of mesh which depends on the parameters of interest is presented in this paper. This was done by adopting reasonable mesh interval sizes. The results of the test cases affirmed the consistency of the condition. It becomes clear that, in general both parameters of interest are linearly related in each case, and the piecewise-uniform mesh number is doubled that of the uniform mesh in order to obtain realistic solution.

Copyright © 2020 PENERBIT AKADEMIA BARU - All rights reserved

1. Introduction

1.1 The General Model

General model of problem is defined in differential form as

$$Lu := -\epsilon\varphi'' + b(x)\varphi' + c(x)\varphi = f(x), \text{ for } x \in (0,1), \quad (1)$$

* Corresponding author.

E-mail address: aslam@uthm.edu.my (Aslam Abdullah)

<https://doi.org/10.37934/cfdl.12.8.108120>

with the boundary conditions

$$\varphi(0) = 0, \varphi(1) = 1, \tag{2}$$

and the assumptions

$$\begin{aligned} \epsilon &> 0, \\ b(x) &> 0 \text{ for all } x \in [0,1], \\ c(x) &\geq 0 \text{ in } [0,1], \end{aligned}$$

where $-\epsilon\varphi''$ is diffusive, $b(x)\varphi'$ is convective, $c(x)\varphi$ is reactive and $f(x)$ is source/sink terms. The functions $b(x)$, $c(x)$, and $f(x)$ are sufficiently smooth. Applying the transform of variable $x \rightarrow (1-x)$, the problem in Eq. (1) still remains when $b(x) < 0$ in $[0,1]$. Note that only when $b(x) \neq 0$ for all $x \in [0,1]$ does Eq. (1) become important with regard to convection. When $\epsilon \ll \|b\|_{L^\infty(\Omega)}$, the parameter ϵ is defined as singular perturbation parameter, and the problem is said to be singularly perturbed. In the case where there are no convection, reaction and source, Eq. (1) represents the pure diffusion process where the solution is linear in space, which is not our interest here.

The consistency and stability of the finite difference technique are compromised when ϵ is small, due to the influence of a boundary layer which appears generally in the solution of Eq. (1) and Eq. (2) at $x = 1$. The consistency of the technique could be improved provided that one chooses the boundary values in such a way that no boundary layer exists. This, however, does not guarantee the stability of the technique [1,2]. In this paper, $c(x) = f(x) = 0$ is considered where Eq. (1) reduces to

$$Lu := -\epsilon\varphi'' + b(x)\varphi' = 0, \text{ for } x \in (0,1), \tag{3}$$

involving an unknown parameter φ . In the case of convection-diffusion problem, for instance, diffusion causes φ as scalar concentration to spread, while convection carries it along with the moving fluid element [3,4]. The sharp change of φ in space occurs after it initially grows slowly over a defined distance when ϵ is small, given appropriate boundary conditions. The sudden rise of φ serves two numerical purposes; to test severely the method of discretization, and the selection of compatible computational domain mesh structure.

1.2 Issues on Mesh Structures

There are major issues on mesh structures that draw research attentions. These include the influence of mesh on numerical accuracy and mesh's effectiveness in reducing the computation time [5-17] in solving a governing equation. Minimization of mesh number, mesh refinement or un-refinement, two-mesh schemes [17-19], multimesh methods [20-25], and spurious oscillation [26] are among mesh concepts that receive wide attentions in the research field.

Lattice Boltzmann scheme (LBS) performs at a similar level as Lax-Wendroff scheme of the one-step second-order with respect to simulation time decrease [5,10]. The scheme is even better than that of projection method based finite difference.

In a study by Yuezhen *et al.*, [13], the employment of an operator interpolation scheme, Richardson extrapolation technique usage, and the application of a fourth-order compact difference scheme were involved in an extensive numerical procedure to solve convection-diffusion equation on the fine mesh with sixth-order accuracy. Other high-order-accuracy schemes corresponding to such equation were also proposed in some studies [9,14].

The improper decrease of mesh number may cause spurious oscillation. One of the successful methods is that of component-wise splitting [7]. The method which is an absolutely stable finite difference scheme greatly decreases mesh number of the analysis system by introducing the irregular mesh size. In addition to clear illustration of the problem of oscillation, it was proposed in previous studies [26,27] that severe oscillations in the solution of convection dominated diffusion equation could be decreased by means of the upwind hybrid difference method which has been improved. It is also worth to note that Superbee, MINMOD, and SMART were shown to be effective in producing physically realistic calculation results. These second-order discretization schemes were evaluated in a previous study [12] where ‘unphysical solution’ term was coined to portray a more general problem.

In this paper, the model problem in Eq. (3) which may be considered as a ‘special’ convection-diffusion problem is discretized by finite difference technique on two types of mesh, i.e. uniform and Shishkin meshes; a piecewise equidistant mesh is defined in such a way that it is sufficiently fine in a neighborhood of $x = 1$. Note that the mesh of Shishkin type is considered to represent the piecewise-uniform mesh. There is a need to prevent φ profile from being nonphysical by determining a valid minimum mesh number. In order to achieve physically realistic solution of the flow problem with less pre-computation time, the flow parameter of interest ϵ in Eq. (3) is examined in connection with mesh number N . The work is an extension to that on mesh and low Peclet numbers’ relationship that was discussed in previous studies [28,29]. Since the solutions are at the risk of being nonphysical, the reduction of mesh number needs to be done with care.

Fluid dynamists have undoubtedly studied various types of mesh, yet comparative study between the uniform and piecewise-uniform meshes corresponding to the condition for preventing spurious oscillatory solutions of singularly perturbed problem remains open. It is important to study such condition to appreciate the appropriateness of these types of mesh in solving the governing equation of interest, thus eradicate some heuristic parts in numerical computation. This research aims at providing a qualitative guideline to avoid nonphysical solutions on both meshes.

2. Methodology

2.1 Discretization

Defining the boundary conditions of the model problem represented by Eq. (3) as

$$\begin{aligned}\varphi(0) &= 0 \\ \varphi(1) &= 1,\end{aligned}\tag{4}$$

uniform mesh and that of piecewise-uniform (represented by Shishkin mesh) are considered to cover the corresponding solution domain. The numerical analysis results support the use of these mesh types. Given that the mesh number N to be an odd integer. The number of interval is thus given by $(N - 1)$. Defining x to be the independent variable whose domain is discretized (i.e. $x = [0,1]$), the nodes in both meshes were defined as follows. In the case of uniform mesh, the node is simply defined as

$$x_{i+1} = x_i + \frac{1}{N - 1},$$

for the nodes x_0, \dots, x_{N-1} , while in that of Shishkin mesh, the node is given by

$$x_{i+1} = x_i + \frac{2}{N-1} - 2r_e \frac{\ln(N-1)}{N-1},$$

for the nodes $x_0, \dots, x_{(N-1)/2}$, and

$$x_{i+1} = x_i + 2r_e \frac{\ln(N-1)}{N-1},$$

for the nodes $x_{(N-1)/2}, \dots, x_{N-1}$, where $0 \leq i \leq (N-1), i \in \mathbb{Z}$, and the parameter $r_e > 0$. Thus there are several intervals, namely a uniform sized intervals Δx_A in uniform mesh, and two sized intervals (i.e. Δx_B and Δx_C) in that of Shishkin type depending on the nodes.

In the mesh of Shishkin type, the meeting point between the coarse and the very fine mesh is known as the transition point. Its location is given by

$$x = x_{(N-1)/2} = r_e \ln(N-1)$$

Clearly $\sum \Delta x_i = 1$. The meshes are illustrated in Figure 1 and Figure 2 below.



Fig. 1. Computational molecules in uniform mesh



Fig. 2. Computational molecules in Shishkin mesh which represents the piecewise-uniform mesh

The idea is to discretize Eq. (3) such that the partial derivatives are approximated by nodal algebraic expression. Thus for every single node, there is an algebraic version of Eq. (3), where the variables to be determined are those at that and instant nodes. The system of algebraic equations is given by

$$C_P \varphi_P + \sum_m C_m \varphi_m = Q_p \tag{5}$$

where P denotes the nodes at which the algebraic equations are allocated, while m index runs over the immediate left and right nodes. The elements of the corresponding matrix C in Eq. (5) are stored as three $n \times n$ array. They are non-zeros only on the matrix's main diagonal (represented by C_{ii}) as well as the diagonals immediately below and above it (represented by C_L and C_R , respectively). Using the three-point computational molecules, Eq. (5) becomes

$$C_P \varphi_P + C_R \varphi_{i+1} + C_L \varphi_{i-1} = Q_P \tag{6}$$

Discretization of all terms in Eq. (3) is done by using central difference scheme (CDS), both for the outer derivative in the first term

$$-[(\epsilon \varphi')']_i \approx \frac{(\epsilon \varphi')_{i+\frac{1}{2}} - (\epsilon \varphi')_{i-\frac{1}{2}}}{\frac{1}{2}(x_{i-1} - x_{i+1})} \tag{7}$$

and the inner derivative

$$\left. \begin{aligned} (\epsilon\varphi')_{i+\frac{1}{2}} &\approx \epsilon \frac{\varphi_{i+1}-\varphi_i}{x_{i+1}-x_i} \\ -(\epsilon\varphi')_{i-\frac{1}{2}} &\approx \epsilon \frac{\varphi_i-\varphi_{i-1}}{x_{i-1}-x_i} \end{aligned} \right\} \quad (8)$$

as well as the second term in Eq. (3)

$$-[(b\varphi)']_i \approx b \frac{\varphi_{i+1}-\varphi_{i-1}}{x_{i-1}-x_{i+1}} \quad (9)$$

The contributions of the first and second terms to the coefficients of the algebraic Eq. (6) are therefore

$$\begin{aligned} C_R &= C_R^{second} + C_R^{first} \\ &= \frac{b}{x_{i+1}-x_{i-1}} - \frac{2\epsilon}{(x_{i+1}-x_{i-1})(x_{i+1}-x_i)}; \\ C_L &= C_L^{second} + C_L^{first} \\ &= -\frac{b}{x_{i+1}-x_{i-1}} - \frac{2\epsilon}{(x_{i+1}-x_{i-1})(x_i-x_{i-1})}; \\ C_P &= C_P^{second} + C_P^{first} \\ &= -(C_R^{first} + C_L^{first}) \end{aligned}$$

Linearization is not required by the numerical solution of Eq. (3). This is due to the linearity of the differential equation, thus the approximate equation contains only terms which are linear. The linear system of the algebraic Eq. (6) is solved by applying Thomas' algorithm (i.e. tridiagonal matrix algorithm). It is set that

$$b = 1.0, r_e = .03 \quad (10)$$

Illustration in Figure 3 shows the nonphysical solution of Eq. (3) where spurious oscillation occurs due to improper minimization of the number of mesh N . Note that the negative values for the solution on Shishkin mesh are magnified 10^{32} times for enhanced visibility. The symbols N_s and N_u represent Shishkin and uniform mesh numbers, respectively. It is therefore necessary to find a technique that is systematic rather than heuristic to use in the determination of N .

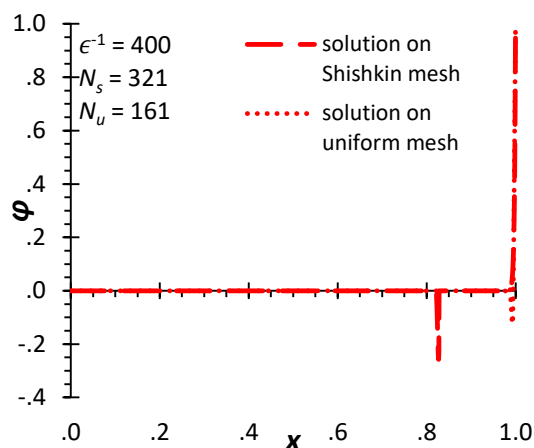


Fig. 3. The insufficient mesh number leads to nonphysical behaviour of φ profile over computational domain; physically correct profile is not supposed to have negative values

2.2 Sequences of ϵ^{-1} and the Mesh Number

The connection between ϵ^{-1} and mesh number N is represented by a set of ordered pairs $((\epsilon^{-1})_i, N_i), i = 1, 2, \dots, n$. The range of ϵ^{-1} of interests is $[50, 1600]$. A sequence of ϵ^{-1} is defined by

$$\begin{aligned} &(\epsilon^{-1})_i, \\ &(\epsilon^{-1})_{i+1} = (\epsilon^{-1})_i/p, \\ &(\epsilon^{-1})_{i+2} = (\epsilon^{-1})_{i+1}/p, \end{aligned} \tag{11}$$

$$(\epsilon^{-1})_n = (\epsilon^{-1})_{n-1}/p,$$

where the constants $i, p \in \mathbb{Z}^+$. Next, defining a sequence of N by

$$\begin{aligned} &N_i, \\ &N_{i+1} = \frac{N_i + 1}{q} - \frac{(-1)^{\left(\frac{N_i+1}{q}+1\right)} - 1}{2}, \\ &N_{i+2} = \frac{N_{i+1}+1}{q} - \frac{(-1)^{\left(\frac{N_{i+1}+1}{q}+1\right)} - 1}{2}, \end{aligned} \tag{12}$$

$$N_n = \frac{N_{n-1} + 1}{q} - \frac{(-1)^{\left(\frac{N_{n-1}+1}{q}+1\right)} - 1}{2},$$

where the constants $i, q \in \mathbb{Z}^+$. Let

$$\begin{aligned} &i = j = 1, n = 6, (1/\epsilon)_1 = 1600, N_1 = 1281, \text{ and} \\ &p = q = 2, \end{aligned} \tag{13}$$

such that the sequence in Eq. (11) and Eq. (12) become

1600, 800, 400, 200, 100, 50

and

1281, 641, 321, 161, 81, 41

respectively.

2.3 Spatial Error Growth Model

Substituting Eq. (7), Eq. (8), and Eq. (9) into Eq. (3);

$$\frac{\varphi_{i+1}-\varphi_{i-1}}{2\epsilon} = \frac{\varphi_{i+1}-2\varphi_i+\varphi_{i-1}}{\Delta x} \quad (14)$$

The spatial error is defined as

$$\gamma = \mathcal{N} - E \quad (15)$$

where \mathcal{N} and E are finite accuracy numerical solution from a real computer and exact solution of difference equation, respectively. Note that the numerical solution \mathcal{N} satisfies the difference Eq. (14). A Fourier series model can be used to analytically represent the random variation of γ with respect to space;

$$\gamma(x) = \sum_l e^{\alpha x} e^{ik_l x}, l = 1, 2, 3 \dots, \quad (16)$$

where $e^{\alpha x}$ is the amplification factor, k_l is the wave number, and α is a constant.

Lets $e^{\alpha x}$ in Eq. (16) be proportional to x when numerical oscillation occurs. Thus it is sufficient to consider only the growth of $e^{\alpha x}$. Direct substitution of $e^{\alpha x}$ into the finite difference Eq. (14) gives

$$\frac{e^{\alpha(x+\Delta x)} - e^{\alpha(x-\Delta x)}}{2\epsilon} = \frac{e^{\alpha(x+\Delta x)} - 2e^{\alpha x} + e^{\alpha(x-\Delta x)}}{\Delta x} \quad (17)$$

In order to have a non-growing error amplification, the criterion

$$\frac{e^{-\alpha\Delta x}(\Delta x + 2\epsilon) - 4\epsilon}{\Delta x - 2\epsilon} \leq 1 \quad (18)$$

must be fulfilled. Note that Eq. (18) is obtained after manipulating Eq. (17). The details can be found in a study by Aslam [28].

3. Result and Discussion

Rewriting Eq. (18) in terms of ϵ and N ;

$$\frac{e^{-\frac{\alpha}{N-1}\left(\frac{1}{N-1}+2\epsilon\right)-4\epsilon}}{\frac{1}{N-1}-2\epsilon} \leq 1 \tag{19}$$

Define

$$G = \frac{e^{-\frac{\alpha}{N-1}\left(\frac{1}{N-1}+2\epsilon\right)-4\epsilon}}{\frac{1}{N-1}-2\epsilon} \tag{20}$$

Thus Eq. (19) becomes

$$G \leq 1 \tag{21}$$

If the mesh is uniform, then $\frac{1}{N-1}$ is constant. However, the term has two values when the Shishkin mesh is considered. In such case, the larger one is chosen. In particular, Eq. (20) becomes

$$G_u = \frac{e^{-\frac{\alpha}{N_u-1}\left(\frac{1}{N_u-1}+2\epsilon\right)-4\epsilon}}{\frac{1}{N_u-1}-2\epsilon}; \tag{22}$$

$$G_s = \frac{e^{-\frac{\alpha}{N_s-1}\left(\frac{1}{N_s-1}+2\epsilon\right)-4\epsilon}}{\frac{1}{N_s-1}-2\epsilon}, \tag{23}$$

where the subscript u and s indicates uniform and Shishkin meshes, respectively. The criterion in Eq. (22) and Eq. (23) were checked against all 36 possible pairs $((\epsilon^{-1})_i, N_j)$ per type of mesh, respectively, based on sequences in Eq. (11) and Eq. (12). The output is given in Table 1, where the shaded cells indicate cases for $G \leq 1$.

Table 1

Range of grid numbers N that fulfils the criterion in Eq. (21) where $\alpha = -0.1$

| N | $\epsilon^{-1} = 1600$ | | $\epsilon^{-1} = 800$ | | $\epsilon^{-1} = 400$ | | $\epsilon^{-1} = 200$ | | $\epsilon^{-1} = 100$ | | $\epsilon^{-1} = 50$ | |
|------|------------------------|-------|-----------------------|-------|-----------------------|-------|-----------------------|-------|-----------------------|-------|----------------------|-------|
| | G_s | G_u | G_s | G_u | G_s | G_u | G_s | G_u | G_s | G_u | G_s | G_u |
| 1281 | ≤ 1 | ≤ 1 | ≤ 1 | ≤ 1 | ≤ 1 | ≤ 1 | ≤ 1 | ≤ 1 | ≤ 1 | ≤ 1 | ≤ 1 | ≤ 1 |
| 641 | > 1 | > 1 | > 1 | > 1 | > 1 | > 1 | > 1 | > 1 | > 1 | > 1 | > 1 | > 1 |
| 321 | | | | > 1 | > 1 | > 1 | > 1 | > 1 | > 1 | > 1 | > 1 | > 1 |
| 161 | | | | | | > 1 | > 1 | > 1 | > 1 | > 1 | > 1 | > 1 |
| 81 | | | | | | | | > 1 | > 1 | > 1 | > 1 | > 1 |
| 41 | | | | | | | | | | > 1 | > 1 | > 1 |

For $\epsilon^{-1} = 50$, all uniform mesh numbers Eq. (12) are appropriate in achieving physically accurate non-oscillatory solutions. This is indicated by G_u being less than or equal to 1. The appropriate range of N_u shrinks by one element each time the previous ϵ^{-1} in Eq. (11) is considered.

Meanwhile, all Shishkin mesh numbers but $N_s = 41$ in Eq. (12) are sufficient to obtain realistic solutions for $\epsilon^{-1} = 50$, where G_s is smaller than or equals 1. The range of sufficient N_s gets smaller by one element every time the previous ϵ^{-1} in Eq. (11) is given except when $\epsilon^{-1} = 1600$; for both $\epsilon^{-1} = 800$ and $\epsilon^{-1} = 1600$, $N_s = 1281$.

The values of G tabulated in Table 1 were verified by plotting φ against x as shown in Figure 4, where the profiles change exponentially with respect to x -direction, and the area below the curve

represented by the integral $\int_0^1 \varphi(x) dx$ is inversely proportional to ϵ^{-1} . The plots which are validated against that in Figure 5 show correct physical behaviors of the solutions. It is confirmed now that in any case where $G \leq 1$, the spurious oscillations can be avoided, and the amplitudes grow with respect to x when $G > 1$.

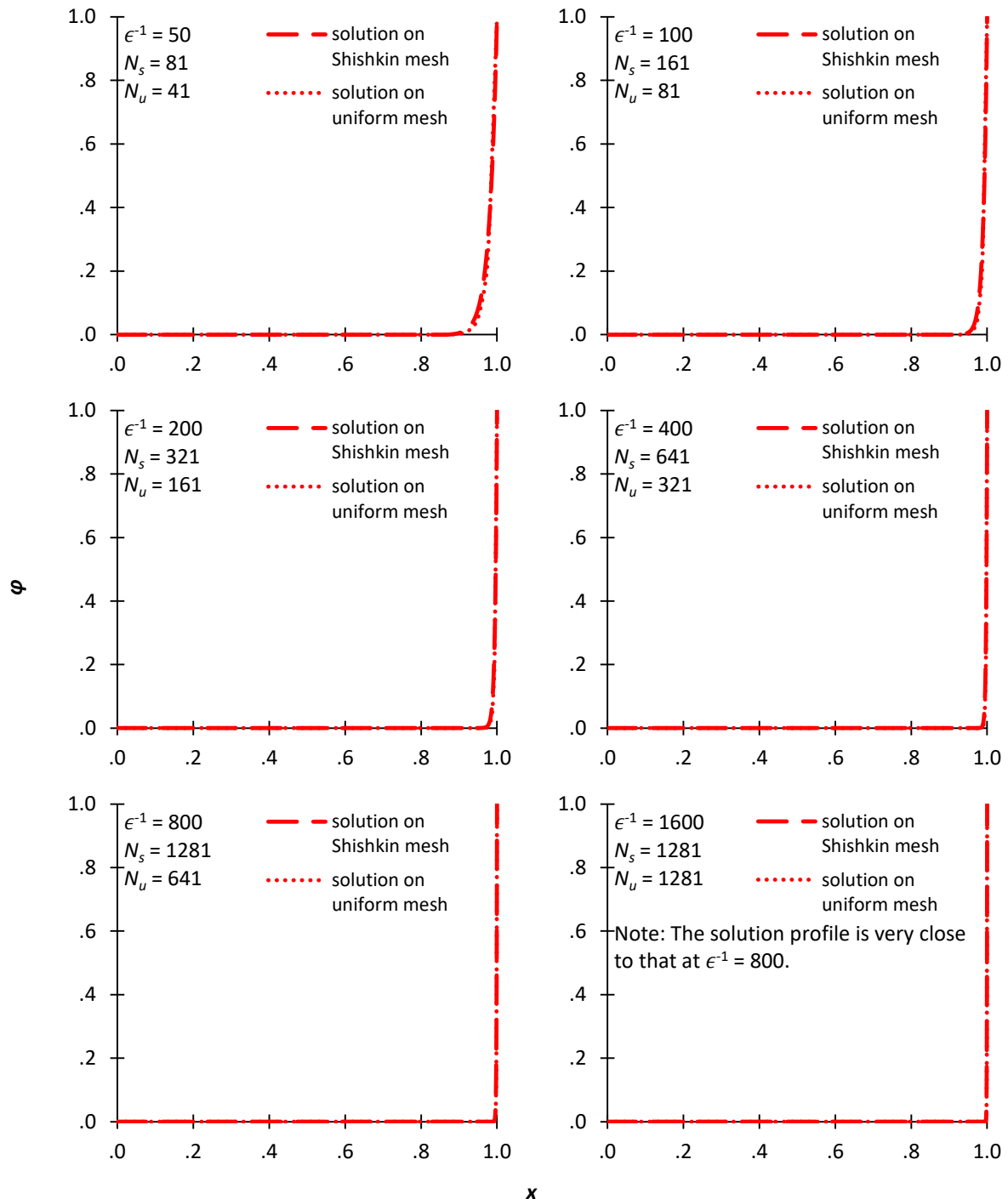


Fig. 4. The solution profile at $\epsilon \ll 1$, numerically calculated, where dash and dot lines represent solutions on Shishkin and uniform meshes, respectively

There are several findings in this numerical calculation of a singularly perturbed two-point boundary value problem. Firstly, the minimum uniform mesh number $N_{u_{min}}$ is linearly proportional

to ϵ^{-1} for $\epsilon^{-1} \in [50,1600]$, while $N_{s_{min}}$ is for $\epsilon^{-1} \in [50,800]$. Thus, the minimum mesh number N_{min} for solving problem in Eq. (3), with the conditions in Eq. (4), is expressed as a linear function of ϵ^{-1} ;

$$N_{min} = m\epsilon^{-1} + d \text{ for } 50 \leq \epsilon^{-1} \leq 1600, \tag{24}$$

corresponding to uniform mesh, where m and d are curve slope and a constant, respectively, and

$$N_{min} = \tilde{m}\epsilon^{-1} + \tilde{d} \text{ for } 50 \leq \epsilon^{-1} \leq 800, \tag{25}$$

corresponding to Shishkin mesh, where \tilde{m} and \tilde{d} are curve slope and a constant, respectively.

Secondly, there is an intersection between both $\epsilon^{-1}N_{min}$ relationships. In particular, it is found that $N_{u_{min}} = N_{s_{min}}$ when $\epsilon^{-1}=1600$. These are clearly seen in Figure 6.

Thirdly, as shown in Figure 6, N_{min} must be sufficient for the φ profile to behave physically correctly. In other words, if $N < N_{min}$ for the corresponding ϵ^{-1} , where N in an element in Eq. (12), then the solution would oscillate as, for instance, depicted previously in Figure 3. If $N \geq N_{min}$, the solution is physically correct.

Forthly, in general, the number of uniform mesh (i.e. $N_{u_{min}}$) is approximately half that of Shishkin mesh (i.e. $N_{s_{min}}$) such that the solution is realistic. Thus, the red dots curve slope m in Figure 6 is half that of black dots, \tilde{m} .

The illustration in Figure 5 shows the theoretical φ profiles for three ranges of b/ϵ . Note that in this paper, the profile of interest is that when $b/\epsilon > 0$. It is clear that the correct solutions are non-negatives and do not oscillate. Thus the profiles in Figure 4 and that in Figure 5 are in agreement when $b/\epsilon > 0$.

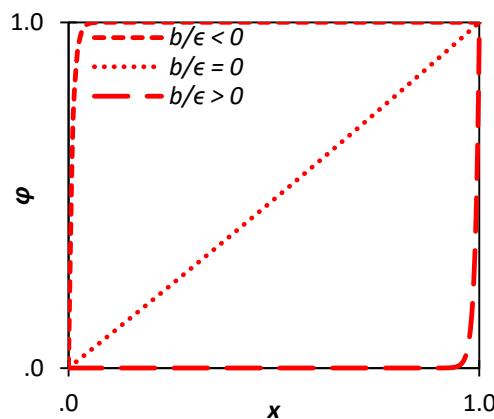


Fig. 5. Solution profiles for different ranges of b/ϵ where boundary conditions are fixed

4. Conclusions

A comparative study of the condition to avoid spurious oscillation in the solution of a singularly perturbed problem on the uniform mesh and that of piecewise-uniform which is represented by the Shishkin mesh has been performed. The condition represents a qualitative guideline that improves our understanding on the contribution of pair (ϵ^{-1}, N) to the oscillation, where ϵ and N are singular perturbed parameter and mesh number, respectively. Interestingly to note that the condition as given in Eq. (21) is applicable not only for the solution on a uniform mesh as discussed in a study by

Aslam [28], but also a piecewise-uniform mesh; it gives the values of N below which non-physical solutions occur.

The solution on the uniform mesh reflects that the linear relationship between both parameters of interest (i.e. ϵ and N) is wider in comparison to that on the piecewise-uniform mesh as revealed in Figure 6.

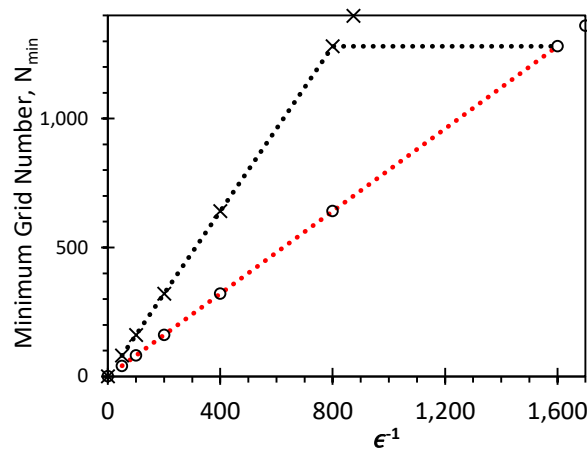


Fig. 6. Minimum mesh number N_{min} as a linear function of ϵ^{-1} , where 'x' and 'o' represent linear relation 1 and 2, respectively, while black and red dots denote numerical relations corresponding to Shishkin and uniform meshes, respectively

It has also been proven in this paper that there is a common value of ϵ^{-1} where both types of mesh can no longer be distinguished with regard to the mesh number N . Furthermore, in general the usage of the uniform mesh can reduce 50% of the mesh number compared to the piecewise-uniform mesh.

Acknowledgement

The author would like to thank Universiti Tun Hussein Onn Malaysia (UTHM) and Ministry of Higher Education of Malaysia (MoHE) for the research facilities. This research is supported by Research Fund E15501 under Research Management Centre, UTHM.

References

- [1] Ferziger, Joel H., and M. Perić. "Properties of numerical solution methods." *Computational Methods for Fluid Dynamics* 3, no. 2 (2002): 31-35.
<https://doi.org/10.1007/978-3-642-56026-2>
- [2] John, Volker. "Numerical Methods for Scalar Convection-Dominated Problems." 2013.
- [3] Abdullah, Aslam. "Mathematical relationship between grid and low Peclet numbers for the solution of convection-diffusion equation." *ARPJ. Eng. Appl. Sci* 13, no. 9 (2018): 3182-3187.
- [4] Abdullah, Aslam. "Grid number and expansion factor for the solution of scalar convection-dominated equation: comparison between the method of 'shooting' and that of finite-difference." *ARPJ. Eng. Appl. Sci* 15, no. 2 (2020): 215-224.
- [5] Ying Hu, Dong Zhang, Jianzheng Yuan, Shaojian Huang, Di Yao, Ling Xu, Cai Zhang, and Qianqing Qin. "An efficient multi-scale waveform inversion method in Laplace-Fourier domain." *Petroleum Exploration and Development* 42, no. 3 (2015): 369-378.
[https://doi.org/10.1016/S1876-3804\(15\)30027-6](https://doi.org/10.1016/S1876-3804(15)30027-6)

- [6] Su, Yan, and Jane H. Davidson. "A Non-Dimensional Lattice Boltzmann Method for direct and porous medium model simulations of 240-tube bundle heat exchangers in a solar storage tank." *International Journal of Heat and Mass Transfer* 85 (2015): 195-205.
<https://doi.org/10.1016/j.ijheatmasstransfer.2015.01.109>
- [7] Shoumei, Xiong, F. Lau, and W. B. Lee. "An efficient thermal analysis system for the die-casting process." *Journal of materials processing technology* 128, no. 1-3 (2002): 19-24.
[https://doi.org/10.1016/S0924-0136\(02\)00029-8](https://doi.org/10.1016/S0924-0136(02)00029-8)
- [8] Van der Sman, R. G. M., and M. H. Ernst. "Convection-diffusion lattice Boltzmann scheme for irregular lattices." *Journal of Computational Physics* 160, no. 2 (2000): 766-782.
<https://doi.org/10.1006/jcph.2000.6491>
- [9] Xu, Mingtian. "A type of high order schemes for steady convection-diffusion problems." *International Journal of Heat and Mass Transfer* 107 (2017): 1044-1053.
<https://doi.org/10.1016/j.ijheatmasstransfer.2016.10.128>
- [10] Cotronis, Yiannis, Elias Konstantinidis, Maria A. Louka, and Nikolaos M. Missirlis. "A comparison of CPU and GPU implementations for solving the Convection Diffusion equation using the local Modified SOR method." *Parallel Computing* 40, no. 7 (2014): 173-185.
<https://doi.org/10.1016/j.parco.2014.02.002>
- [11] Xiong, S. M., F. Lau, W. B. Lee, and L. R. Jia. "Numerical methods to improve the computational efficiency of thermal analysis for the die casting process." *Journal of materials processing technology* 139, no. 1-3 (2003): 457-461.
[https://doi.org/10.1016/S0924-0136\(03\)00553-3](https://doi.org/10.1016/S0924-0136(03)00553-3)
- [12] Guenther, C., and M. Syamlal. "The effect of numerical diffusion on simulation of isolated bubbles in a gas–solid fluidized bed." *Powder Technology* 116, no. 2-3 (2001): 142-154.
[https://doi.org/10.1016/S0032-5910\(00\)00386-7](https://doi.org/10.1016/S0032-5910(00)00386-7)
- [13] Ma, Yuezhen, and Yongbin Ge. "A high order finite difference method with Richardson extrapolation for 3D convection diffusion equation." *Applied Mathematics and Computation* 215, no. 9 (2010): 3408-3417.
<https://doi.org/10.1016/j.amc.2009.10.035>
- [14] Ge, Lixin, and Jun Zhang. "High accuracy iterative solution of convection diffusion equation with boundary layers on nonuniform grids." *Journal of Computational Physics* 171, no. 2 (2001): 560-578.
<https://doi.org/10.1006/jcph.2001.6794>
- [15] Abdullah, Aslam. "Grid expansion factor for the shooting method solution of convection-diffusion equation." *ARPN J. Eng. Appl. Sci.* 14, no. 7 (2019): 1370-1376.
- [16] Qin, Xin-qiang, and Yi-chen Ma. "Two-grid scheme for characteristics finite-element solution of nonlinear convection diffusion problems." *Applied mathematics and computation* 165, no. 2 (2005): 419-431.
<https://doi.org/10.1016/j.amc.2004.06.021>
- [17] Weng, Zhifeng, Jerry Zhijian Yang, and Xiliang Lu. "Two-grid variational multiscale method with bubble stabilization for convection diffusion equation." *Applied Mathematical Modelling* 40, no. 2 (2016): 1097-1109.
<https://doi.org/10.1016/j.apm.2015.06.023>
- [18] Yang, Daoqi. "A characteristic mixed method with dynamic finite-element space for convection-dominated diffusion problems." *Journal of computational and applied mathematics* 43, no. 3 (1992): 343-353.
[https://doi.org/10.1016/0377-0427\(92\)90020-X](https://doi.org/10.1016/0377-0427(92)90020-X)
- [19] Zhang, Jun, Lixin Ge, and Jules Kouatchou. "A two colorable fourth-order compact difference scheme and parallel iterative solution of the 3D convection diffusion equation." *Mathematics and Computers in simulation* 54, no. 1-3 (2000): 65-80.
[https://doi.org/10.1016/S0378-4754\(00\)00205-6](https://doi.org/10.1016/S0378-4754(00)00205-6)
- [20] Dai, Ruxin, Jun Zhang, and Yin Wang. "Multiple coarse grid acceleration for multiscale multigrid computation." *Journal of Computational and Applied Mathematics* 269 (2014): 75-85.
<https://doi.org/10.1016/j.cam.2014.03.021>
- [21] Ge, Yongbin, and Fujun Cao. "Multigrid method based on the transformation-free HOC scheme on nonuniform grids for 2D convection diffusion problems." *Journal of Computational Physics* 230, no. 10 (2011): 4051-4070.
<https://doi.org/10.1016/j.jcp.2011.02.027>
- [22] Goldstein, C. I. "Preconditioned iterative methods for convection diffusion and related boundary value problems." *Computers & Mathematics with Applications* 19, no. 8-9 (1990): 11-29.
[https://doi.org/10.1016/0898-1221\(90\)90261-H](https://doi.org/10.1016/0898-1221(90)90261-H)
- [23] Oosterlee, Cornelis Willebrordus. "The convergence of parallel multiblock multigrid methods." *Applied numerical mathematics* 19, no. 1-2 (1995): 115-128.
[https://doi.org/10.1016/0168-9274\(95\)00020-U](https://doi.org/10.1016/0168-9274(95)00020-U)

-
- [24] Mohamed, S. A., N. A. Mohamed, AF Abdel Gawad, and M. S. Matbuly. "A modified diffusion coefficient technique for the convection diffusion equation." *Applied Mathematics and Computation* 219, no. 17 (2013): 9317-9330.
<https://doi.org/10.1016/j.amc.2013.03.014>
- [25] Sun, Haiwei, Ning Kang, Jun Zhang, and Eric S. Carlson. "A fourth-order compact difference scheme on face centered cubic grids with multigrid method for solving 2D convection diffusion equation." *Mathematics and computers in Simulation* 63, no. 6 (2003): 651-661.
[https://doi.org/10.1016/S0378-4754\(03\)00095-8](https://doi.org/10.1016/S0378-4754(03)00095-8)
- [26] Jeon, Youngmok, and Mai Lan Tran. "The upwind hybrid difference methods for a convection diffusion equation." *Applied Numerical Mathematics* 133 (2018): 69-82.
<https://doi.org/10.1016/j.apnum.2017.12.002>
- [27] Jamal, Muhamad Hafiz Md, and Azlin Mohd Azmi. "Flow past two interlocking squares cylinder at low Reynolds number." *Journal of Advanced Research in Fluid Mechanics and Thermal Sciences* 44, no. 1 (2018): 140-148.
- [28] Abdullah, Aslam. "Condition for non-oscillatory solution for scalar convection-dominated equation." *CFD Letters* 12, no. 4 (2020): 24-34.
<https://doi.org/10.37934/cfdl.12.4.2434>
- [29] Abdullah, Aslam. "Obtaining grid number for the shooting method solution of convection-diffusion equation." *International Journal of Mechanical Engineering, & Technology (IJMET)* 9, no. 5 (2018): 916-924.